Determination of High-Energy Fragmentation of Protonated Peptides Using a BEqQ Hybrid Mass Spectrometer

Odile Burlet,*,† Ralph S. Orkiszewski,* and Simon J. Gaskell*
Center for Experimental Therapeutics,* Baylor College of Medicine, and Department of Chemistry,† University of Houston, Houston, Texas, USA

A hybrid tandem instrument of BEqQ geometry was used to determine high-energy decomposition of protonated peptides, such as side-chain fragmentation yielding d_n and w_n ions. The transmission through both E and Q of such product ions, formed in the second field-free region, permits improved mass resolution and confident mass assignment. The experimental technique may involve synchronous scanning of E and Q, or, for the purpose of identification of specific products, limited-range scanning of either E or Q with the other analyzer fixed. These techniques are not equivalent, with respect to product ion transmission, to the double focusing of product ions achieved with four-sector instruments but nevertheless represent a critical improvement over conventional mass-analyzed ion kinetic energy spectrometry analyses. Fragmentation of protonated peptides occurring in the second field-free region inside and outside the collision cell were distinguished by floating the collision cell above ground potential. Mass filtering using Q confirmed the mass assignments. The data indicate that product ions resulting from spontaneous decomposition are in some instances quantitatively more significant than those resulting from high-energy collisional activation. Furthermore, the differentiation of the products of low- and high-energy processes should facilitate spectral interpretation. *(J Am Soc Mass Spectrom 1993, 4, 470–476)*

Many important contributions to the structure elucidation of peptides have now been reported using tandem mass spectrometry with either low- or high-energy collisional activation, using (as examples) triple quadrupole [1, 2] and four-sector [3–6] instruments, respectively. Both analytical regimes yield product ion spectra that include fragment ions derived from cleavage of petptide bonds, although the maximum molecular mass for which useful low-energy product ion spectra may be obtained is generally observed to be lower than the limit for the high-energy experiment [7, 8]. It is becoming increasingly clear that the structural features that promote low-energy fragmentation differ from those that favor high-energy cleavages. Thus, for example, amino acid sequences that promote or mitigate charge localization exert an important influence on product ion spectra resulting from low-energy, charge-directed decomposition (either collision activated or spontaneous) [9, 10]. In contrast, high-energy collision-activated decomposition (CAD) product ion spectra include substantial contributions from decompositions that are either necessarily charge remote or may be envisaged to be so. Such fragmentations include side-chain cleavages to yield product ions of the w_n and d_n types (depending on whether charge retention is on the C- or N-terminus, respectively) [11]. (The Biemann variant [3] of the Roepstorff and Fohlman nomenclature [12] for peptide fragmentation is used throughout this study.) The lack of observation of side-chain fragmentation constitutes a significant disadvantage of low-energy CAD, particularly for the differentiation of leucine and isoleucine residues.

Tandem mass spectrometers of hybrid design (BEqQ or EBqQ, where B is the magnetic sector, E the electric sector, q the radiofrequency (RF)-only quadrupole or other multipole, and Q the quadrupole mass filter) are generally used with relatively low energy (tens to hundreds of electron volts) collisional activation (CA) in q. Alexander et al. [13] demonstrated that collision energies (laboratory frame-of-reference) of several hundred electron volts, with helium as target gas, permitted the detection of side-chain fragmentations of peptides, albeit with a considerable sacrifice in transmission through the quadrupole assembly. Transmission of higher kinetic energy ions may be improved by operating q with a higher RF amplitude [14]. Recent analyses of peptides using a hybrid instrument modified in this way, and using a heavier target gas to increase the center-of-mass collision energy, showed some improvement in the detection of side-chain fragmentations of peptides [15]; however, such analyses differ from typical high-energy CAD experiments (such

Address reprint requests to Simon J. Gaskell, Department of Chemistry, UMIST, P.O. Box 88, Manchester M60 1QD, UK.

1044-0305/93/$6.00

Received December 29, 1992
Revised February 15, 1993
Accepted February 16, 1993

as those performed on four-sector instruments) with respect to the time available for decomposition and the multiplicity of collisions.

High-energy (kiloelectron volt) CAD analyses may be performed on a BEqQ hybrid instrument via collisions in the first or second field-free regions [16, 17]. If good resolution of both precursor and product ions is required, the preferred form for the experiment is an extension of a mass-analyzed ion kinetic energy spectrometry (MIKES) analysis, with improved resolution of product ions achieved by mass filtering using Q. This may be accomplished, for example, by using linked E/Q scanning [18, 19]. It is important to recognize that this experiment is not equivalent to a B_2/E_2 linked scan on a four-sector instrument in which the double focusing of product ions is reflected in signal intensity. In contrast, E/Q scanning of the hybrid instrument effectively samples a portion of each MIKES peak. Furthermore, the E/Q scan requires reliable tracking of several potentials [20] (although experimental modifications [21–23] may reduce these requirements). Nevertheless (as data presented later in this study exemplify), the E/Q scanning method can generate useful data from the high-energy CAD of peptides. In addition, experimentally less demanding approaches can also exploit the mass-resolving capabilities of the quadrupole to define the mass-to-charge ratios of specific product ions formed in the second field-free region following high-energy CAD. One method [16] consists of selecting the mass-to-charge ratio of the candidate fragment ion using Q and scanning a narrow range of E. The other approach [16] selects the kinetic energy/charge ratio of the relevant ion using E and scans Q to define mass-to-charge ratio values with unit resolution.

During CAD/MIKES analyses, the selected precursor ion is induced to fragment by collision in the gas cell between B and E. Additionally, spontaneous (metastable) decomposition processes may occur throughout this field-free region. A product ion spectrum acquired in this manner therefore represents the combined result of high-energy CAD and low-energy metastable processes. The contributions of the fragmentations occurring inside and outside the collision cell can be separated by applying a potential to the gas collision cell [24–26]. When the collision cell is at ground potential, the kinetic energy E_2 of a product ion of mass m_2 formed at any point in the second field-free region is given by eq 1 (assuming negligible kinetic energy losses),

$$E_2 = (m_2/m_1)zeV_a \quad (1)$$

where V_a is the accelerating voltage of the ion source, m_1 the mass of the precursor ion, z the charge number of the precursor ion, and e the charge of one electron. When the collision cell is floated at a potential V_c, the kinetic energy E_2' of the same product ion formed by CAD in the gas collision cell is given by eq 2:

$$E_2' = (m_2/m_1)ze(V_a - V_c) + zeV_c \quad (2)$$

The kinetic energy of product ions formed by spontaneous decomposition of the precursor ion in the second field-free region, but outside the collision cell, is still given by eq 1. Thus, distinction can be made, on the basis of location in the MIKE spectrum, between ions formed inside the collision cell (principally by CAD) and outside the cell (mainly by spontaneous decomposition). Further refinement of the experiment may be achieved using a BEqQ instrument by consecutive energy and mass-to-charge ratio analysis of product ions.

MIKES analyses with a potential applied to the gas collision cell were initially performed using double-focusing instruments to study specific CAD processes (see, for example, refs 24–29). Floating the gas collision cell was subsequently shown to improve resolution of product ions [18] and increase the transmission efficiency of low-mass (relative to the precursor) product ions transmitted through the electric sector analyzer [30]. Following the development of four-sector ($[E_1, B_1]/[E_2, B_2]$) tandem mass spectrometry, the use of a floated cell in high-energy CA analyses is now commonplace. The linked scan law governing B_2 and E_2 is invariably established to achieve transmission of product ions formed within the collision cell.

In the present study, high-energy (kiloelectron volt) fragmentations of peptide $[M + H]^+$ ions were determined using several analytical modes on a BEqQ hybrid mass spectrometer. The relative contributions of low- and high-energy processes occurring during CAD/MIKES analyses of protonated peptides were assessed; the data have significant implications for high-energy CAD analyses performed on other instrument types.

Experimental

Materials

Glucagon (22–29) and angiotensin III were purchased from Bachem Inc. (Torrance, CA). Ser-Ile-Gly-Ser-Leu-Ala-Lys was from Sigma Chemical Co. (St. Louis, MO). Synthetic Glu-Glu-Leu-Cys-Thr-Met-Phe-Ile-Arg and Gly-Phe-Leu-Cys-Gly-His-Tyr-Arg (prepared using standard procedures) were kindly provided by Drs. J. T. Sparrow and R. Cook (Baylor College of Medicine, Houston, TX), respectively. [Interest in these peptides arises from a parallel study (to be published) of the tryptic fragments of human apolipoprotein B-100.] Hydrogen peroxide 30% (Fisher Scientific Co., Fair Lawn, NJ) and formic acid (J. T. Baker Chemical Co., Phillipsburg, NJ) were used as received. Oxidation of Glu-Glu-Leu-Cys-Thr-Met-Phe-Ile-Arg was performed as described previously [9].

Mass Spectrometry

One to five micrograms of peptide was used for each analysis. All analyses were performed using a VG ZAB SEQ hybrid mass spectrometer (VG Analytical Ltd., Manchester, UK) of BEqQ geometry. Ionization by fast-atom bombardment used xenon atoms with energies of 8 keV as the primary beam. The liquid matrix used was a 1:1 mixture of thioglycerol/2,2'-dithiodiethanol (2-hydroxyethyl disulfide), saturated with oxalic acid. (This matrix is customarily used in this laboratory for all peptide analyses; alternative matrices were not specifically evaluated for the present study.) The accelerating voltage was 8 kV. Low-energy CAD product ion spectra used argon as collision gas at an estimated pressure of $2–3 \times 10^{-4}$ mbar, corresponding to an attenuation of 50–60% of the precursor ion intensity. The collision energy was 12–15 eV in the laboratory frame of reference. High-energy CAD analyses used argon as collision gas in the second field-free region collision cell, at a pressure sufficient to decrease the precursor ion beam by 50–80%. For certain experiments, the collision cell potential was set at 500 V. Product ion spectra were acquired via the VG 11-250 data system in "multichannel analyzer" mode. Scans were of 15-s duration, and 9–20 scans were accumulated. Specific scan modes are described at appropriate points in the following section.

Results and Discussion

Using the hybrid BEqQ instrument, low-energy CAD product ion spectra were obtained by selecting $[M + H]^+$ precursor ions at the point of double focus, inducing decomposition in q, and analyzing the product ions by scanning the mass analyzer quadrupole (Q). The low-energy CAD spectrum of Ser-Ile-Gly-Ser-Leu-Ala-Lys (SIGSLAK) is shown in Figure 1. Extensive fragmentation gave both C- and N-terminal fragment ions corresponding to single cleavages of the peptide backbone (a_n, b_n, and y_n types). Product ions (such as the d_n or w_n series) associated with concurrent cleavages of the peptide backbone and of side chains were absent from the low-energy product ion spectrum. The high-energy CAD product ion spectrum of SIGSLAK $[M + H]^+$, acquired using MIKES, is presented in Figure 2. Numerous C- and N-terminal fragment ions were observed, including apparent d_n and w_n ions arising from side-chain fragmentation. The possible presence of d_5 and w_6 ions was of particular interest because these would be associated with leucine and isoleucine residues, respectively. The effective mass resolution of the product ions in the MIKES analysis, however, was not sufficient to ensure confident assignments. To confirm the presence of d_5 and w_6 ions in the MIKE spectrum, each individual MIKES peak of interest was mass analyzed using the quadrupole mass filter (Q). The first set of experiments consisted of performing a MIKES analysis with Q set to transmit only one mass-to-charge ratio value. Figure 3 compares an analysis of this type with the result for conventional MIKES analysis; the data confirm the detection of the w_6 ion, m/z 543, derived from the isoleucine residue at the 2-position. Equivalent analyses (Figure 4) confirmed the presence of a d_5 ion at m/z 388, associated with the leucine at residue 5. Less prominent signals observed in Figures 3b and 4b corresponding to product ions of greater than expected kinetic energy were attributed to fragmentation processes (yielding the same mass-to-charge ratio product ions) occurring in the RF-only quadrupole. Another set of experiments was then performed to determine the homogeneity (with respect to mass-to-charge ratio) of the MIKES peaks attributed to d_5 and w_6 ions. For these analyses, Q was scanned with E static to transmit ions of kinetic energy corresponding to the maxima of the

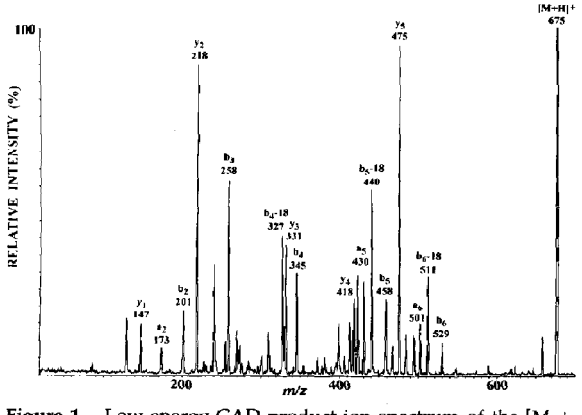

Figure 1. Low-energy CAD product ion spectrum of the $[M + H]^+$ ion of SIGSLAK at m/z 675. [Decompositon in q, with a collision energy (laboratory frame of reference) of 12 eV.]

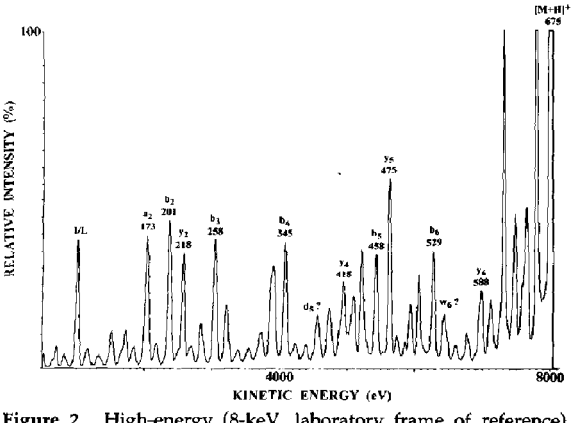

Figure 2. High-energy (8-keV, laboratory frame of reference) CAD/MIKE spectrum of the $[M + H]^+$ ion of SIGSLAK at m/z 675. (Decomposition in the second field-free region; collision cell at ground potential.) I/L, immonium ion derived from the leucine or isoleucine residues.

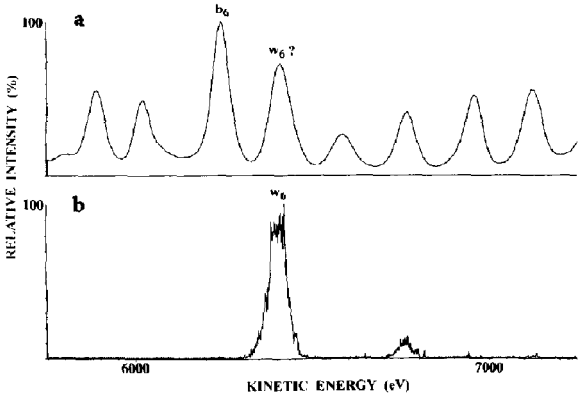

Figure 3. High-energy CAD of SIGSLAK $[M + H]^+$, m/z 675; scanning of product ions in the region of the putative w_6 ion formed in the second field-free region: (a) detection following E; (b) detection after selection of ions of m/z 543 using Q.

MIKES peaks apparently attributable to the w_6 ion (Figure 5a) or the d_5 ion (Figure 5b). The single peak detected in Figure 5a at m/z 543 again confirmed the presence of the w_6 ion and also suggested that no other product ion contributed to the MIKES peak. The MIKES peak, which included the d_5 product ion, however, was shown to have multiple origins (Figure 5b). The d_5 assignment was substantiated by the presence of the peak at m/z 388, but other ions of m/z 385–389 were also reproducibly observed, indicating that MIKES analysis alone provides insufficient mass resolution for confident assignment of these product ions. The relative abundances of product ions of m/z 385–389 cannot be inferred from Figure 5b because the contributions from each species will vary across the MIKES peak.

A similar series of experiments to those described above were conducted with another leucine-containing peptide: Gly-Phe-Leu-Cys-Gly-His-Tyr-Arg

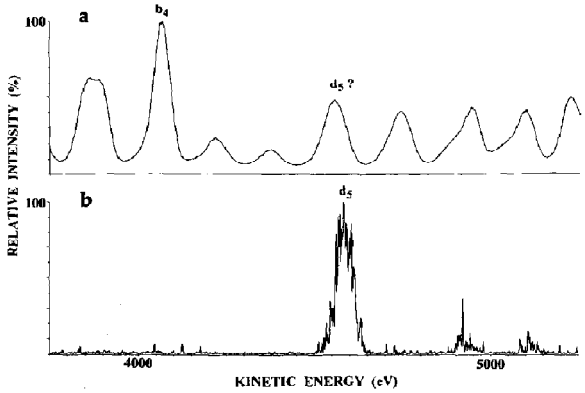

Figure 4. High-energy CAD of SIGSLAK $[M + H]^+$, m/z 675; scanning of product ions in the region of the putative d_5 ion formed in the second field-free region: (a) detection following E; (b) detection after selection of ions of m/z 388 using Q.

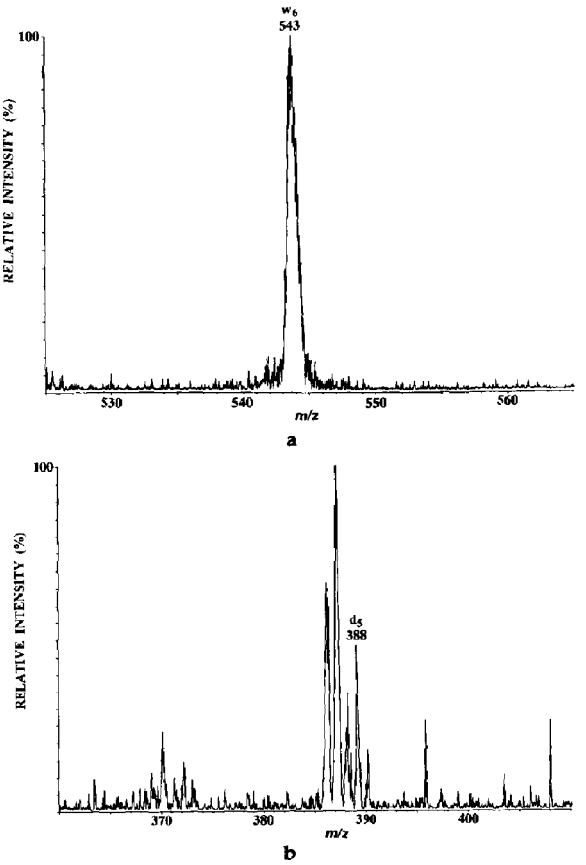

Figure 5. Narrow-range Q scans following high-energy CAD in the second field-free region of the $[M + H]^+$ ion of SIGSLAK: (a) E set to transmit 6443 eV, corresponding to the putative w_6 ion; (b) E set to transmit 4604 eV, corresponding to the putative d_5 ion.

(GFLCGHYR). The low-energy CAD product ion spectrum of GFLCGHYR included informative sequence ions (a_n, b_n, and y_n) but no side-chain fragment ions (d_n or w_n). The CAD/MIKE product ion spectrum of GFLCGHYR also displayed sequence ions (a_n, b_n, and y_n), together with apparent w_n ions, including the w_6 species associated with the leucine residue at position 3. The assignment of the w_6 (m/z 689) ion was confirmed by the detection of a single peak of the expected kinetic energy when E was scanned with Q set to transmit m/z 689. Scanning of Q with E set to transmit the MIKES peak corresponding to the w_6 ion suggested that the MIKES peak was homogeneous.

The relative contributions of high-energy CAD and spontaneous decomposition processes occuring during such MIKES analyses of peptide $[M + H]^+$ ions were assessed by floating the MIKES collision cell above ground potential. The MIKE spectrum of Glu-Glu-Leu-cysteic acid-Thr-methionine sulfone-Phe-Ile-Arg (EELC*TM*FIR) acquired in the absence of collision

gas is shown in Figure 6a. The entire series of y ions was observed except y_8. This spectrum was similar to the low-energy CAD product ion spectrum acquired by decomposition of the precursor ion in q [9]. The CAD/MIKE spectrum of EELC*TM*FIR, recorded with the collision cell at ground potential, is presented in Figure 6b. The y_n series of ions was again prominent, and, additionally, w_n ions were observed (albeit with low abundance with respect to the lower members of the series). Comparison of these two spectra (Figure 6a, b) confirmed that w ions were products of high-energy CAD [11]. The CAD/MIKE spectrum of EELC*TM*FIR acquired with the MIKES cell floated at 500 V is presented in Figure 6c. The w_n ions were shifted to kinetic energy values higher than those in Figure 6b; the magnitudes of the shifts were as predicted by eq 2. The assignment of the w_6 ion was confirmed by mass-to-charge ratio-deconvoluted MIKES analyses; Figure 7 shows narrow-range MIKES analyses performed with Q set to transmit m/z 753 for the w_6 ion. The spectra in Figure 7a,b were acquired with the MIKES collision cell at ground potential and floated at 500 V, respectively. The single peak detected at 4940 eV in Figure 7a confirmed the presence of the

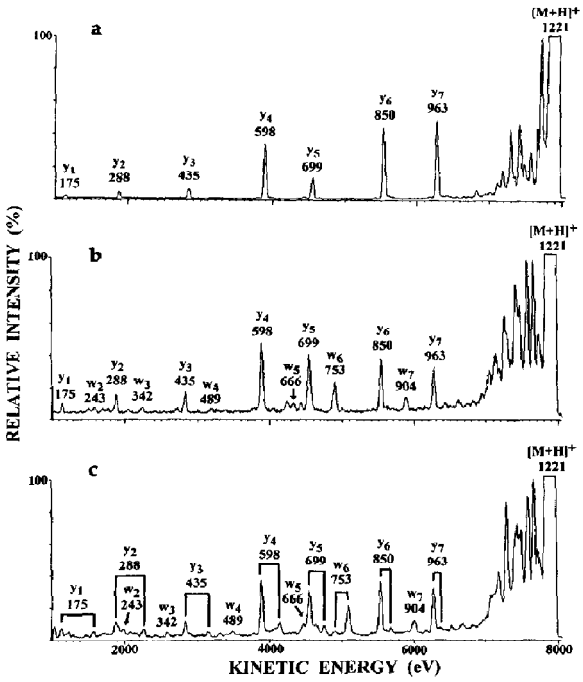

Figure 6. Product ion spectra (E scans) of decompositions of EELC*TM*FIR (where C* is cysteic acid, and M* is methionine sulfone) $[M + H]^+$, occurring in the second field-free region, with detection after E: (**a**) no collision gas; (**b**) CAD with the collision cell at ground potential; (**c**) CAD with the collision cell at 500 V. **Brackets** indicate the presence of product ions of the same mass-to-charge ratio but different kinetic energy/charge ratios, arising from their origins inside or outside the collision cell.

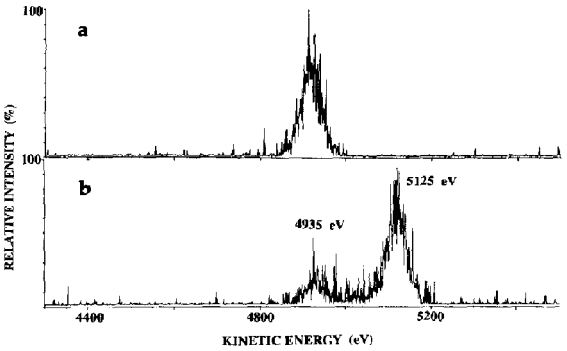

Figure 7. High-energy CAD of the $[M + H]^+$ ion of EELC*TM*FIR (C* and M* are as in Figure 6); mass-to-charge ratio-deconvoluted MIKE spectra with Q set to transmit m/z 753, corresponding to the w_6 ion: (**a**) collision cell at ground potential; (**b**) collision cell floated at 500 V.

w_6 ion associated with the leucine at position 3. The prominent peak detected at 5130 eV when the collision cell was floated (Figure 7b) indicated that the w_6 ion was mainly formed in the collision cell by high-energy CAD processes. The presence of a residual signal at 4935 eV in Figure 7b indicated that a minor proportion of w_6 ions (which were not observed in the absence of collision gas; Figure 6a) were formed outside the collision cell. Two possible explanations are proposed for this observation. First, the w_6 ions formed outside the cell may result from CA, with gas leaking from the cell. Second, CA within the cell may be followed by delayed fragmentation occurring outside the cell. It has been emphasized previously [27] that unimolecular and bimolecular processes can be clearly distinguished by floating the collision cell only if ion–molecule reactions take place exclusively in the collision cell.

In Figure 6c, two peaks are observed for each y_n ion, one at the same kinetic energy value (eq 1) as in Figure 6b and the other at a higher value predicted by eq 2. The peak of unchanged kinetic energy is the more intense for all y_n ions. Mass-to-charge ratio-deconvoluted MIKES analyses were performed with Q set to transmit m/z 699 for the y_5 ion and with the collision cell at ground potential and floated at 500 V (Figure 8). The single peak observed at 4585 eV with the grounded cell was also prominent when the cell was floated. A small peak was detected at a higher kinetic energy value (4800 eV) corresponding to y_5 ions formed in the collision cell. A minor intermediate signal appeared at an approximate kinetic energy/charge ratio consistent with fragmentation in the collision cell of the y_6 ion, itself formed in the field-free region immediately preceding the cell. These data indicate that for the example of this peptide, the most abundant ions observed in the CAD/MIKES experiment result principally from low-energy processes occurring outside the collision cell.

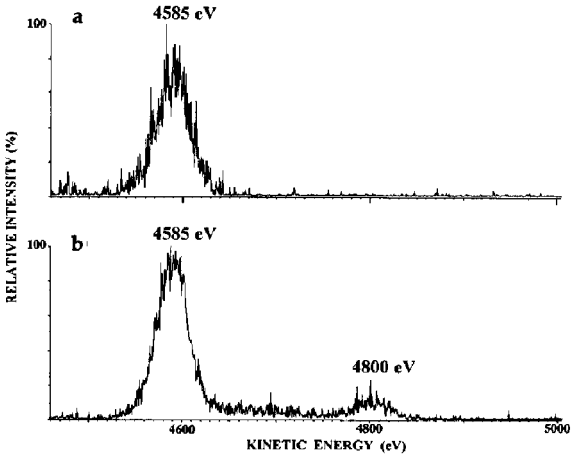

Figure 8. High energy CAD of the $[M + H]^+$ ion of EELC*TM*FIR (C* and M* are as in Figure 6); mass-to-charge ratio-deconvoluted MIKE spectra with Q set to transmit m/z 699, corresponding to the y_5 ion: (a) collision cell at ground potential; (b) collision cell floated at 500 V.

Similar approaches were followed in the analyses of other synthetic peptides. Analyses of angiotensin III, Arg-Val-Tyr-Ile-His-Pro-Phe (RVYIHPF), provided information on the formation of N-terminal ions. The metastable MIKE spectrum of RVYIHPF included series of b_n ions (b_3–b_6), a_n ions (a_2–a_5), and y_n ions (y_2–y_6). The addition of gas to the collision cell enhanced the relative abundances of a_n ions and generated a series of d_n ions (d_2–d_4 and d_7), together with two immonium ions from the histidine and tyrosine residues. Comparison of the MIKE spectra acquired under metastable and CA conditions indicated that d_n ions (as well as immonium ions in this case) were entirely the result of CA processes. The CAD/MIKES analysis of angiotensin III performed with the collision cell floated at 500 V showed a shift in the kinetic energy value for all d_n ions, confirming their formation in the collision cell via high energy CA processes. The peaks corresponding to b_n ions were of unchanged kinetic energy, showing their formation outside the gas collision cell via low-energy processes. The peaks corresponding to a_n ions were split into two components (indicating dual origins inside and outside the collision cell), with proportions differing among members of the ion series.

The CAD/MIKES analyses of glucagon (22–29), Phe-Val-Gln-Trp-Leu-Met-Asn-Thr, produced abundant b_n ions. Comparison of the spectra obtained with the grounded and floated collision cell showed that the b_n ions possessed the same kinetic energy in both cases, consistent with the conclusion from the angiotensin III results that product ions of this type result from low-energy processes.

Linked scanning of E and Q, with and without floating of the MIKES collision cell, provides an alternative experimental approach to the determination of the contribution of low-energy decomposition processes to spectra recorded in a CAD/MIKES analysis. In the experiments described here, the scan law applied for E/Q linked scanning was the same whether the collision cell was floated or not. Thus, when the MIKES collision cell was at ground potential, ions formed anywhere in the second field-free region were detected. When the collision cell was floated, only ions formed outside the collision cell were detected; ions formed inside the floated collision cell possessed increased kinetic energies (eq 2), and their transmission through Q was therefore defeated by the E/Q link. Thus, by eliminating ions formed in the collision cell via high-energy CA processes, the E/Q linked scan spectrum with a floated cell represents the contribution from ions formed outside the collision cell. Figure 9a,b shows the E/Q linked scans of EELC*TM*FIR acquired under CAD conditions with the MIKES collision cell at ground potential and floated at 500 V, respectively. The spectrum in Figure 9a display two series of ions (y_3–y_7 and w_5–w_7). (Some discrimination against low mass-to-charge ratio members of the y_n series is evident and is attributed to the difficulty of maintaining the appropriate E/Q and high-voltage links across a broad range.) The same y_n series was observed when the collision cell was floated (Figure 9b), but the abundances of the w_n ions were markedly reduced. For the same reasons as previously discussed with the CAD/MIKES experiments (Figure 6), the minor residual peaks corresponding to w_n ions observed with the floated cell can be attributed to ions formed outside the collision cell following CA.

It may be noted that high-energy CA analyses using four-sector instruments frequently use a collision cell floated above ground potential. A complex scan law governing B_2 and E_2, determined by the float potential, is applied [31] to allow detection of product ions formed within the cell so that the procedure discrimi-

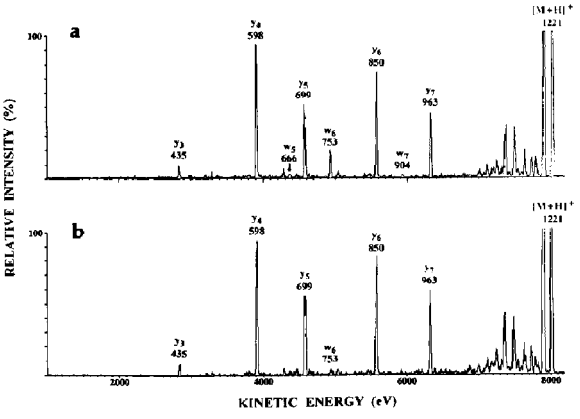

Figure 9. E/Q-linked scans recorded with high-energy CAD in the second field-free region of the $[M + H]^+$ ion, m/z 1221, of EELC*TM*FIR (C* and M* are as in Figure 6): (a) collision cell at ground potential; (b) collision cell floated at 500 V.

nates against detection of the products of low-energy processes. Complementary scanning with B_2/E_2 constant would of course conversely discriminate against detection of the products of CA to produce a spectrum similar to that recorded in the absence of collision gas. The discrimination against certain fragment types observed with some scan modes (whether on hybrid or four-sector instruments) may be turned to interpretive advantage in facilitating the recognition of particular ion series.

In summary, the consecutive kinetic energy- and mass-resolving capabilities of a BEqQ hybrid mass spectrometer were used to determine the fragmentations of protonated peptides occurring in the region between B and E. By permitting satisfactory mass resolution of both precursor and product ions in the tandem mass spectrometry experiment, this approach represents an important extension of the capabilities of a double-focusing instrument, although it does not match the transmission achieved using four-sector instruments (and therefore implies a substantially greater sample requirement). The independent kinetic energy and mass resolution of product ions achieved with the hybrid have also been used to assess the contributions of low-energy fragmentation processes to the composite product ion spectra recorded under high-energy CAD conditions. Floating the collision cell in the region between B and E revealed that for the synthetic peptides examined, the products of low-energy processes (such as y_n and b_n ions) made quantitatively major contributions to the spectra recorded. When a floated cell is used, the scan mode selected (on either a hybrid or four-sector instrument) influences the relative transmission efficiencies of the products of low- and high-energy processes, permitting a potentially useful discrimination among fragment types.

Acknowledgment

This work was supported by the National Institutes of Health (GM 48267).

References

1. Hunt, D. F.; Yates, J. R. III; Shabanowitz, J.; Winston, S.; Hauer, C. R. *Proc. Natl. Acad. Sci. USA* **1986**, *83*, 6233–6237.
2. Hunt, D. F.; Shabanowitz, J.; Yates, J. R.; Griffin, P. R.; Zhu, N. Z. In *Mass Spectrometry of Biological Materials*; McEwen, C. N.; Larsen, B. S., Eds.; Marcel Dekker: New York, 1990; p 169.
3. Biemann, K. *Biomed. Environ. Mass Spectrom.* **1988**, *16*, 99–111.
4. Biemann, K. In *Methods in Enzymology*, Vol. 193; McCloskey, J. A., Ed.; Academic: San Diego, CA, 1990; p 455.
5. Burlingame, A. L.; Walls, F. C.; Falick, A.; Evans, S.; Riddoch, A.; Buchanan, R. *Rapid Commun. Mass Spectrom.* **1990**, *4*, 447–448.
6. Carr, S. A.; Anderegg, R. J.; Hemling, M. E. In *The Analysis of Peptides and Proteins by Mass Spectrometry*; McNeal, C. J., Ed.; John Wiley: Chichester, 1988; p 95.
7. Bean, M. F.; Carr, S. A.; Thorne, G. C.; Reilly, M. H.; Gaskell, S. J. *Anal. Chem.* **1991**, *63*, 1473–1481.
8. Alexander, A. J.; Thibault, P.; Boyd, R. K.; Curtis, J. M.; Rinehart, K. L. *Int. J. Mass Spectrom. Ion Processes* **1990**, *98*, 107–134.
9. Burlet, O.; Yang, C.-Y.; Gaskell, S. J. *J. Am. Soc. Mass Spectrom.* **1992**, *3*, 337–344.
10. Burlet, O.; Orkiszewski, R. S.; Ballard, K. D.; Gaskell, S. J. *Rapid Commun. Mass Spectrom.* **1992**, *6*, 658–662.
11. Johnson, R. S.; Martin, S. A.; Biemann, K. *Int. J. Mass Spectrom. Ion Processes* **1988**, *86*, 137–154.
12. Roepstorff, P.; Fohlman, J. *Biomed. Mass Spectrom.* **1984**, *11*, 601.
13. Alexander, A. J.; Thibault, P.; Boyd, R. K. *Rapid Commun. Mass Spectrom.* **1989**, *3*, 30–34.
14. Alexander, A. J.; Dyer, E. W.; Boyd, R. K. *Rapid Commun. Mass Spectrom.* **1989**, *3*, 364–372.
15. Bradley, C. D.; Curtis, J. M.; Derrick, P. J.; Wright, B. *Anal. Chem.* **1992**, *64*, 2628–2635.
16. Clupek, J. D.; Amy, J. W.; Cooks, R. G.; Schoen, A. E. *Int. J. Mass Spectrom. Ion Processes* **1985**, *65*, 141–157.
17. Harrison, A. G.; Mercer, R. S.; Reiner, E. J.; Young, A. B.; Boyd, R. K.; March, R. E.; Porter, C. J. *Int. J. Mass Spectrom. Ion Processes* **1986**, *74* 13–31.
18. Beynon, J. H.; Harris, F. M.; Green, B. N.; Bateman, R. H. *Org. Mass Spectrom.* **1982**, *17*, 55–66.
19. Louris, J. N.; Wright, L. G.; Cooks, R. G.; Schoen, A. E. *Anal. Chem.* **1985**, *57*, 2918–2924.
20. Yost, R. A.; Boyd, R. K. In *Methods in Enzymology*, Vol. 193; McCloskey, J. A., Ed.; Academic: San Diego, CA, 1990; p 154.
21. Guevremont, R. *Rapid Commun. Mass Spectrom.* **1987**, *1*, 19–20.
22. Guevremont, R.; Boyd, R. K. *Int. J. Mass Spectrom. Ion Processes* **1988**, *84*, 47–68.
23. Boyd, R. K.; Dyer, E. W.; Guevremont, R. *Int. J. Mass Spectrom. Ion Processes* **1989**, *88*, 147–160.
24. Wachs, T.; Van De Sande, C. C.; McLafferty, F. W. *Org. Mass Spectrom.* **1976**, *11*, 1308–1312.
25. Beynon, J. H.; Cooks, R. G. *Int. J. Mass Spectrom. Ion Phys.* **1976**, *19*, 107–137.
26. Okuno, K. *Mass Spectrosc.* **1976**, *24*, 107–117.
27. Maquestiau, A.; Van Haverbeke, Y.; De Meyer, C.; Flammang, R. *Org. Mass Spectrom.* **1978**, *13*, 207–208.
28. Dallinga, W.; Nibbering, N. M. M.; Louter, G. J. *Org. Mass Spectrom.* **1981**, *16*, 183–187.
29. Maas, W. P. M.; Nibbering, N. M. M. *Int. J. Mass Spectrom. Ion Processes* **1989**, *95*, 171–198.
30. Boyd, R. K.; Bott, P. A.; Beer, B. R.; Harvan, D. J.; Hass, J. R. *Anal. Chem.* **1987**, *59*, 189–193.
31. Boyd, R. K. *Int. J. Mass Spectrom. Ion Processes* **1987**, *75*, 243–264.